Force analysis of two-dimensional complex (dusty) plasma with the vertical S100 Probe

N.M. Walker, B. Harris, J. Dallas, V. Land, L.S. Matthews, T.W. Hyde. *Center for Astrophysics, Space Physics, & Engineering Research, Baylor University, Waco, Texas. (2010).*

***Abstract*— A vertically oriented, negatively charged Ti probe was inserted perpendicularly with respect to the dust crystal. When a series of waves were propagated through the probe into the dust crystal at various probe potentials, the authors saw attraction of the particles which were furthest away from the probe due to the ion-drag flow force and saw repulsion of the particles nearest the probe due to electrostatic repulsion forces. The charge of the probe can be calculated by deriving a charge formula as a function of Debye length. By utilizing this formula, and plotting the results, more extensive studies of dusty plasma can be performed.**

***Index Terms*—complex dusty plasma, dust and force analysis, GEC RF reference cell, Zyvex S100 probe**

I. Introduction

Approximately 99% of the matter in the Universe exists in a plasma state--an electrified gas with its composite atoms dissociated into positive and negative ions. In the laboratory, specifically, in the Gaseous Electronic Conference (GEC) radio frequency (rf) reference cell, at the CASPER lab, this phenomenon is created by exciting argon gas in a vacuum environment. When manually adding spherical dust into the cell, and illuminating the surface with a laser, one notices the dust crystal levitating via force balance. An electric field generated from the lower electrode in the cell gives an upward force to the complex plasma, while gravity is opposing this force downward. The dust of the complex plasma arranges in a group of one-dimensional hexagonal lattices, this is the dust crystal. The hexagonal lattice structure in which the dust arranges itself is a by-product of energy and charge minimization. The dust crystal is confined by a cutout inserted onto the lower electrode. A radial force directed inward restricts this dust crystal to a potential well.

It was shown in a previously published experiment[4] that a negatively biased wire placed coplanar within the dust crystal lattice had the individual dust particles close to the wire repel the inserted charge while the dust residing farther out radially experiences an attraction to the wire. At the CASPER lab, a similar procedure is followed to that in [4], sinusoidal, triangle, and square waves were propagated longitudinally through the dust crystal in order to reproduce the results with a vertical probe.

By inserting a negatively-charged 99% pure titanium metal probe vertically into the dust crystal, repulsion between the dust and probe is observed, creating a void. Thus the dust in the complex plasma must also be negatively charged. The radius of the void is dependent upon two parameters: the distance from the crystal to the probe and the potential on the probe. The plasma sheath, or the edge of the plasma, involves ions which stream downward colliding with the dust resulting in an ion-drag force. This ion-drag force is thought to be responsible for the attraction seen in the outer layers of the dust crystal.

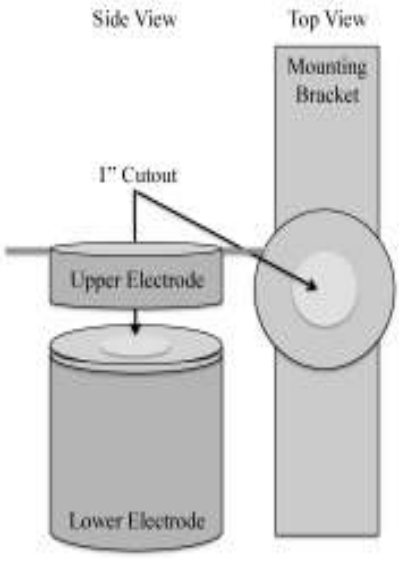

Figure 1.[8] Schematic of cell #2: The electrode position and cutout orientation in the cell used in the CASPER lab. The spacing between the electrodes is 0.75".

In order to study the attraction and repulsion captured by the camera in the cell. A more theoretical approach can be taken by deriving the electrostatic force equation by estimating the charge on the probe.

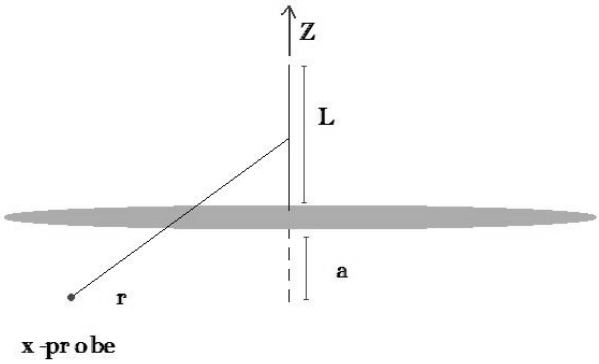

Figure 2. This diagram shows the probe traversing through the dust crystal with a length L, where a is the distance from the tip of the probe to the dust crystal.

The electric potential of the charged particle is given by the following equation:

$$\Phi = \frac{A}{r} e^{\frac{-r}{\lambda_D}} \qquad (1)$$

where r is represented by the relationship: $r = \sqrt{x_p^2 + z^2}$. The first derivative of equation (1) can be taken with respect to z, which gives the electric potential of an infinitesimal piece of the probe. Integrating this over the length of the probe, *l*, gives the electric potential over the entire probe, in the vertical direction.

For the purpose of the study, the electric potential in the x-direction is of particular interest. In order to find the electric field of the probe in the x-direction, the first derivative of the new expression for the electric potential is taken with respect to x (2).

$$Ex_p = - d\Phi/dx \qquad (2)$$

Then, the force exerted in the x-direction by the probe can be calculated by multiplying the charge of the inner-ring dust particle by the electric field in the x-direction.

$$Fx_p = q_{dust} * Ex_p \qquad (3)$$

The forces of the other particles with respect to the inner-ring particle can be determined in a similar fashion by calculating the electric field with respect to the x position of the other dust particles in the crystal.

$$Ex_{dust} = - d\Phi/dx_{dust(i)}$$

from

$$\Phi_i = \frac{q_{dust}}{4\pi\varepsilon_o x_{dust}} e^{\frac{-x_{dusti}}{\lambda_D}}$$

$$Fx_{dust\,(i)} = -q_{dust} * d\Phi/dx_{dust\,(i)} * \cos\theta \qquad (4)$$

where θ is the angle formed between the inner-ring particle, the other dust particles and the probe as seen in figure 3.

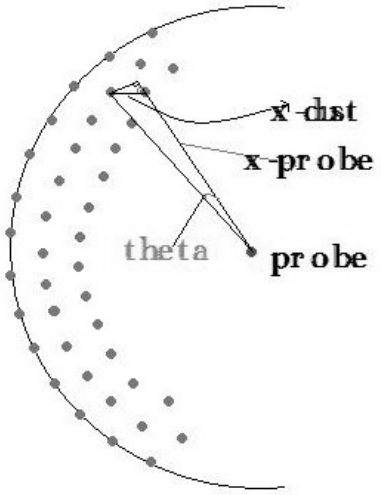

Figure 3. This diagram shows the relationship between the probe and the dust in the dust crystal. From an inner-ring particle, the force of the other dust particles on that inner-ring particle can be calculated by considering the angle theta formed.

Then, the force on the probe in the x-direction can be calculated by performing a summation on (4). Once determined, the charge, q, can be solved for as a function of the Debye length, λ_D (5).

$$q = (A * x_{probe}) \sum_{dust} \left\{ \frac{x_d 4\pi\varepsilon_o e^{\frac{x_d}{\lambda_D}}}{\left(\frac{1}{x_d} + \frac{1}{\lambda_D}\right)\cos\theta} \int_l^{a+l} \left[\frac{z}{(x_p^2 + z^2)^2} * e^{\frac{-\sqrt{x_p^2+z^2}}{\lambda_D}} \left(\frac{3}{\sqrt{x_p^2+z^2}} + \frac{5}{\lambda_D} + \frac{\sqrt{x_p^2+z^2}}{\lambda_D^2} \right) \right] dz \right\}$$

(5)

II. Experimental

A. The GEC RF reference cell

The experiments were performed using a GEC RF reference cell. The cell was used for ease of

experimental duplication in terms of compatibility of multiple laboratory diagnostic measurements. The argon gas was pumped into the cell from an argon gas canister and the line was regulated by a butterfly valve to control the chamber pressure and the mass-flow controller valve to control the flow rate. The power was delivered to the reference cell through the lower electrode via a frequency signal generator held at 13.56 MHz, a variable passive attenuator, and then the signal is fed to an rf amplifier. The voltage and current are measured using an oscilloscope.

The melamine formaldehyde (MF) dust (8.9 μm) was manually inserted using a shaker. The dust is illuminated by a red (636 nm) He-Ne diode laser, class IIIb. The laser beam fanned out horizontally with the width of laser beam 100 microns to 200 microns. The dust crystal was captured by a top-view digital camera at a rate of 60 frames per second.

B. Inserting the probe into the dust crystal to create a void

A series of rf powers (1W, 5W, 10 W), a series of pressures (50 mTorr, 100 mTorr, 300 mTorr, 500 mTorr), and three different probe z-heights (probe at bottom of z-range, probe in-line with crystals, and probe tip at top of side-view) were the parameters varied for this portion of the experiment. As an example: at a power of 10 W, creating a dc bias of -37 V, the probe was vertically inserted into the dust crystal such that the probe tip was in-line with the dust creating a void in the center of the crystal. At this given power, and an Ar gas flow rate of 16 sccm, the pressure inside the cell was adjusted to 50 mTorr. A negative potential voltage was delivered to the probe by a scale of 5 V, from 0 V to -50 V. Because the probe was negatively biased, the dust particles repelled against the probe electrostatically. A series of 12 images were taken for each probe height. These images were stacked and analyzed using the ImageJ software program.

C. Propagating waves longitudinally through the dust crystal

Sinusoidal, square, and triangle waves were propagated through the probe at a series of peak-to-peak voltages (10 V, 30 V, 45 V) at various frequencies (1 Hz, 5 Hz, 10 Hz, 20 Hz, 30 Hz) and at different pressures (50 mTorr, 100 mTorr, 300 mTorr, 500 mTorr). The probe was placed at a height with the tip in-line with the dust crystal. The particle positions were identified and traced over the series of images taken with the top-view camera. These images were processed by using Labview in order to efficiently capture and track the wave propagating through the dust.

D. Image analysis

The images taken from the camera mounted on top of the cell were edited using ImageJ software.

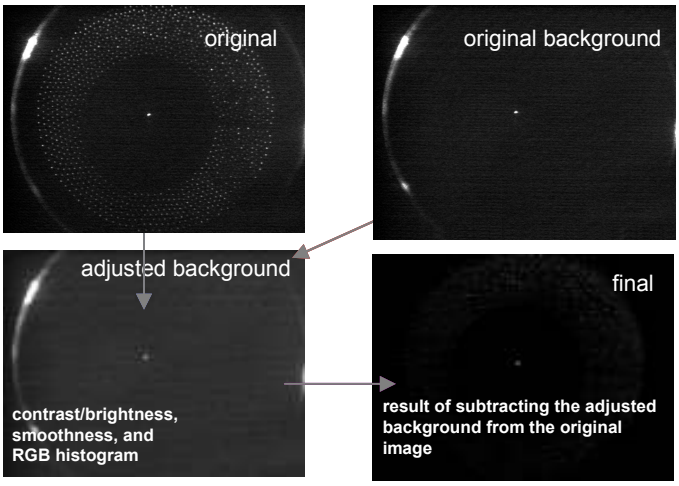

Figure 4. A schematic of the image editing process using the ImageJ software. Starting with the original background image, one adjusts the background and then subtracts the adjusted background from the original image resulting in the final adjusted image.

The importance of editing the images arises when detecting the particles in the dust ring. The software detects bright spots as the dust particles. By only subtracting the original background, the particle detector tracks more particles than those solely in the dust crystal.

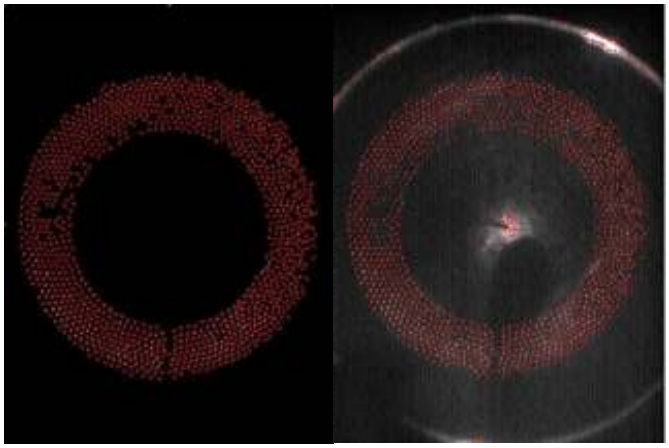

Figure 2. This is a comparison between editing (left) and not editing (right) the background image before running the particle detector in ImageJ.

In figure 2, the ImageJ particle detector ran at the

certain parameters. The average radius of particle to be detected was 3 pixels, the cutoff was 3 pixels, and the percentage of the particles to be detected is 5.0% for the edited image on the left. For the original image on the right, there the parameters used were a radius of 2 pixels, a cutoff 3 pixels, and a percentage 2.2%. By using a particle counter, the total number of particles detected in the original image was 1115, compared to the edited image which detected 1118 particles. Whereas the actual number of particles detected has only a difference of 3 particles, the location of the detected particles is of importance. Notice in the figure on the right, how the particle detector tracked "particles" that are outside of the potential well. The edited image shows more particles in within the dust crystal itself.

III. Results

After editing the images and running the particle detector plug-in with ImageJ, MatLab was used to plot the following graphs which display the size of the void radius dependent upon the probe potential and probe positions with respect to the dust crystal.

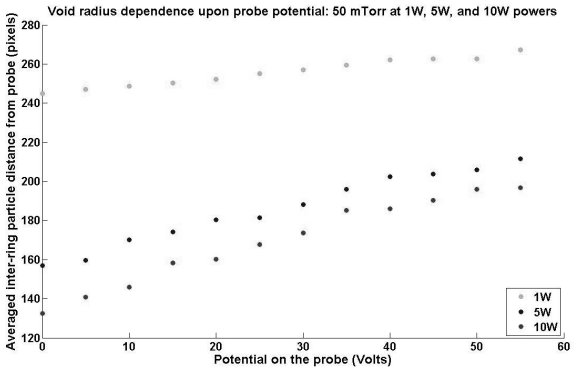

Figure 3. This plot created in MatLab displays the linear progression of void radial size with respect to probe potential at 50 mTorr and three powers: 1W, 5W, 10W.

The linear trend between probe potential and void radial dependence can be seen in figure 3. For the given powers 1W, 5W, and 10W, the average inner-ring particle distance from the probe was calculated for each of the negative probe potential, resulting in a total of 12 data points. The 1W power was scaled to fit the 5W and 10W powers, as the probe potential for the 1W was scaled by intervals of 2V for a series of 0 to -22V. The average starting position (in pixels) when the probe potential is at 0V, is as follows: 1W = 240 pixels, 5W = 159 pixels, and 10W = 135 pixels.

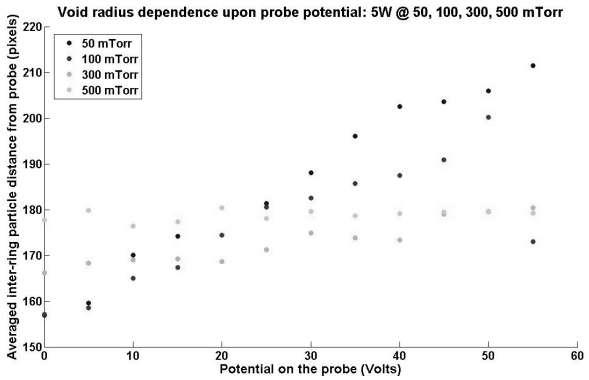

Figure 4. This plot created in MatLab displays the linear progression of void radial size with respect to probe potential at 50 W and four pressures: 50 mTorr, 100 mTorr, 300 mTorr, 500 mTorr.

At a given power and four different pressures, a linear trend is observed. The rate of change of the void radius decreases as the pressure is increased.

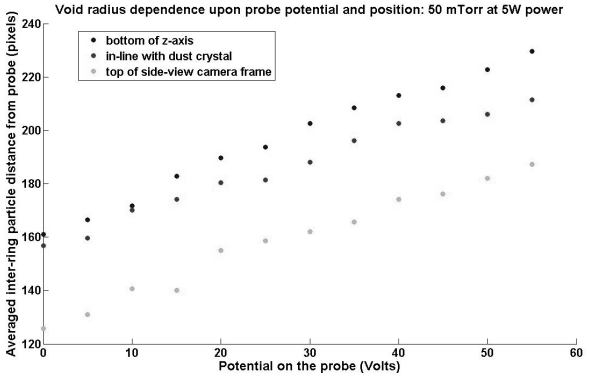

Figure 5. This plot created in MatLab displays the linear progression of void radial size with respect to probe height given a probe potential at 50 mTorr and a power of 5W.

Figure 5. shows the void radial size dependence upon the potential of the probe with respect to each of the given probe heights. The average inter-ring distance from the probe increases with the probe's proximity to the dust crystal. When the probe is below the dust crystal, the average starting void radius is 161 pixels. The radius when the probe is in-line with the dust crystal is 158 pixels. And when the probe is at the top of the side-view camera frame, the void radius is 126 pixels. The linear trend of the radial progression is still observed.

IV. Discussion

The MatLab figures on the previous page all display a linear trend of void radial progression as a function of

probe potential. The linear trends that are observed need to be further investigated

V. CONCLUSIONS

Dropping a negatively charged probe into dust particles causes a void in the center of the dust crystal because the dust is negatively charged. The void size increases radially in a linear fashion was the probe voltage is increased (made more negative). The equation of charge of the probe can be derived and utilized as a function of Debye length in order to further study the characteristics of the dust crystal. Once the data propagation of the waves through a dust crystal has been plotted in order to observe the amplitudes of the waves, the results of this experiment can be compared and contrasted to the results of [4] directly.

Further projects include creating a MatLab program which automates the void imaging process. When the frequency of oscillation is increased to 30 Hz, the waves oscillate out of the plane of the crystal. Thus the waves are propagating in 2-dimensions. The results from this experiment could be very interesting.

ACKNOWLEDGMENT

The authors would like to thank the National Science Foundation for providing funding for the 2010 Summer NSF REU program at the CASPER lab. We would also like to thank Baylor University, the members of the CASPER lab and HIDPL for providing direction and thought-stimulating environment in which to perform this research. We would especially like to thank Jorge Carmona-Reyes, Mike Cook, and Jimmy Schmoke for their sharing their extensive knowledge and expertise.

REFERENCES

[1] M.Zuzic, H.M.Thomas, G.E.Morfill. Wave propagation and damping in plasma crystals. J.Vac.Sci.Technol.A.14.496

[2] J.B.Pieper, J.Goree. Dispersion of plasma dust acoustic waves in the strong-coupling regime. PhysRevLett.77.3137. (1996).

[3] D.Samsonov, J.Goree, et al. Mach cones in a coulomb lattice and a dusty plasma.PhysRevLett.83.3469 (1999).

[4] D.Samsonov. Long-range attractive and repulsive forces in a two-dimensional complex (dusty) plasma. PhysRevE.63.025401 (2001).

[5] B.Harris. REU Proposal: Radial interaction of dust & force analysis with powered Zyvex S100 probe (email communication) (2010).

[6] B.Eliasson, P.K.Shukla. Colloquim: Fundamentals of dust-plasma interactions. Rev. of Modern Physics 81(1) 25(20). (2009).

[7] F.A.Chen. Introduction to Plasma Physics and Controlled Fusion. Volume 1: Plasma Physics. Second Edition.

[8] J.R. Creel, Characteristic Measurements within a GEC RF Reference Cell, (2010).